Keywords
Salivary glands; Histomorphometry; Prosthodontics; Dental materials; Xerostomia

Authors
Firas Riyadh Muhammad[1*]
[1*]Al Ameen university/ college of dentistry Firasriad@gmail.com. Fofenona@gmail.com.

Ali, A. M.[2]
[2]University of baghdad /college of dentistry
ali.abdualrazaq@codental.uobaghdad.edu.iq

Nahidah zaher kamil[3]
[3]Al Ameen university/ college of dentistry Dotnet1375@gmail.com

Received: 11.11.2024
Accepted: 02.05.2025
Doi: 10.1922/ejprd.v34i2.1317

European Journal of Prosthodontics and Restorative Dentistry (2026) 34 (2), 01–12

Structural and Functional Histology of Human Salivary Glands: Clinical Relevance to Prosthodontics and Dental Materials Interaction

ABSTRACT
Human salivary glands are among the most complex exocrine organs, and their histologically organized parenchyma determines the qualitative and quantitative composition of saliva, which is essential for oral homeostasis and long-term prosthetic rehabilitation. This study elucidated the structural and functional histology of the three major human salivary glands using haematoxylin and eosin (H&E) and periodic acid-Schiff (PAS) staining, quantitative histomorphometric analysis, and correlation with salivary functional parameters and pellicle formation on contemporary dental materials. Forty-five human glandular specimens (15 parotid, 15 submandibular, and 15 sublingual) were collected from 15 adult cadavers. Specimens were routinely processed, sectioned, and stained with H&E and PAS. Quantitative morphometric analysis was performed on ten high-power fields, and salivary functional parameters were measured in 60 healthy adult volunteers. Contact angle analysis was also conducted on five categories of dental materials before and after 60 minutes of salivary conditioning. Significant differences were observed among glands in acinar cell morphology, serous-to-mucous acinar ratio, ductal architecture, and PAS-positive secretory granule density. Acinar cell volumetric measurements were positively correlated with stimulated salivary flow volume ($r=0.72$, $p<0.001$). After salivary conditioning, zirconia showed the lowest contact angle and greatest surface free energy, whereas silicone-modified soft liners remained the most hydrophobic. H&E and PAS histomorphic analysis provides meaningful indices of salivary secretory capacity and biomaterial-surface interactions relevant to prosthodontics.

INTRODUCTION
In humans, the salivary glands (parotid, submandibular, and sublingual) are some of the most histologically varied exocrine organs; architectural complexity reflects the variation in salivary activity. Together with the hundreds of minor salivary glands located throughout the oral mucosa, the major salivary glands produce between 0.5 and 1.5 litres of saliva daily in a developing physiological state [1]. The salivary gland consists of a complex combination of water, electrolytes, mucous glycoproteins, digestive enzymes, antimicrobial proteins, growth factors, and immunoglobulins, and the specific composition of this fluid is determined by the histology of the secretory functional cells [2,3]. Thus, the architecturally structured salivary tissue goes beyond simply describing the architecture of salivary gland tissue; it is the biological substrate that utilises the anatomy of the salivary gland as a basis for function specifically salivary gland function, which affects the success of prosthodontic rehabilitation.

The parotid gland is a purely serous exocrine organ that is histologically composed of tightly packed spherical to pyramidal acini, exhibiting abundant basophilic granular cytoplasm, round nuclei located at the basal portion of the cell, and discrete zones of secretory granules located at the apical pole of the cell, as determined by haematoxylin and eosin (H&E) staining.

These serous acinar cells are responsible for producing large quantities of the low-viscosity, enzyme-rich secretion characteristic of the parotid gland during mastication (i.e., primarily alpha-amylase).The histological features of the submandibular salivary gland are mixed in nature, with the majority of the acini being serous in type, however there are also mucous elements to the gland in that tubes containing mucous are capped by a crescentic collection of serous cells called demilunes, thus providing a fair quantity of mucin to the secretion produced by the glands [4]. When sectioned and stained with H&E, the contrast between the deep-stained serous cells, which have many granules, and pale, foamy mucous cells, which are filled with mucin, are the key histological characteristics of the submandibular salivary gland. The sublingual salivary gland represents the other end of the histological spectrum as a predominantly mucous gland. The parenchyma of the sublingual salivary gland consists primarily of mucous acini; the cells of these acini exhibit the characteristic vacuolated pale cytoplasm and flattened nuclei typical of cells that secrete mucin. The sublingual salivary gland also contains demilunes, but they are comparatively minimal in amount [5].

The duct system of the salivary glands is a structurally important component of the architecture of the glands, which is readily identifiable when the glands are sectioned and stained with H&E. Intercalated ducts connect the acinar secretory units to the striated duct system and contain a low cuboidal epithelium with minimal cytoplasm and small, round nuclei. The number of intercalated ducts is proportionately greater in the parotid salivary glands than any of the other major salivary glands [6]. The striated ducts represent the most readily identifiable part of the ductal system, they contain tall columnar cells that have eosinophilic cytoplasm, nuclei that are oriented centrally in the cells, and the basal striations of these cells result from the infolding of the plasma membrane that surrounds rows of elongated mitochondria [7]. The striations in the striated ducts can be seen with high power magnification using H&E; these striations reflect the high energy demands of the ionic pumps located in the striated ducts that modify the primary isotonic secretion and produce and secrete the hypotonic, bicarbonate-rich saliva delivered into the oral cavity.Excretory ducts, which carry modified secretions to the oral cavity, are lined with epithelial cells in layers of varying thickness (pseudostratified, then stratified columnar epithelium; then stratified squamous epithelium) with the largest diameter being at the oral opening [7].

Supportive connective tissue known as stroma, composed of fibroblasts, collagen bundles, reticular fibres, blood vessels, nerves and adipocytes, provides the supporting structure for the lobules of the gland and varies with respect to quantity based on gland type and age. The parotid gland demonstrates a marked age dependent atrophy of the acini and a progressive replacement of the parenchyma with adipocytes, which decrease the functional secretory cell volume while not concomitantly reducing the volume of the gland itself, and is clearly visible on routine H&E sections [8]. Myoepithelial cells (identified on H&E by their flattened, elongated appearance and lightly stained cytoplasm with a spindle-shaped nucleus) form a thin sheet covering the outer surface of each acinus and intercalated duct and produce contractile force under autonomic stimulation to aid in the exiting of secretory products from the acinar lumen [9] The structural integrity of myoepithelial cells, assessed by their continuity and regularity of investment around an acinus, is an important indicator of how effectively the glandular parenchyma mechanically secretes its products.

The periodic acid-Schiff (PAS) stain provides critical complementary information to H&E stained specimens as it provides a means for staining neutral polysaccharides and glycoproteins to a magenta colour due to the conversion of vicinal diols to aldehydes by oxidation with periodic acid and subsequent linkage by Schiff's reagent [10]. Within a salivary gland section, PAS staining demonstrates the mucous secretory granules present in mucous acinar cells and demilune serous cells, the basement membranes surrounding the acini and ducts, and the connective tissue ground substance [11]. The quantity of secretory granules in salivary glands can be analyzed through histological measurements (i.e., number and size) of PAS-positive granule area of acinar salivary epithelial cells (i.e., acini). These two measures represent the immature or mature granule proportions. These two proportions can be measured and used to assess or provide an indication of the acinar cells' secretory reserve capacity through histological means.The forces generated from the interaction of film, surface tension, and viscosity provide resistance to displacement loads applied during function [12]. There is a significant contribution to this resistance by the glycoproteins mucin of submandibular/submandibular secretions. These glycoproteins are responsible for maintaining the salivary film that forms under complete dentures, while also producing interfacial lubrication to help reduce frictional trauma to the mucosa [13]. Patients with reduced saliva due to polypharmacy, head & neck radiation therapy, autoimmune sialadenitis, or aging frequently report instability of their dentures, difficulty wearing their prosthesis long term, and sores on their mucosa. The common thread through all of these issues is mechanistic evidence demonstrating a decrease in the number of secretory acinar cells as shown by histomorphometric analysis [14].

The salivary pellicle is an ordered film of proteins that is applied in several seconds to any intraoral substance, including a prosthesis, and is responsible for altering the surface energy, wettability, and biological compatibility of the substrate in fundamentally (relative to the specific structural and chemical characteristics of prosthetic material) different ways [15]. The proteins of saliva (statherin, proline-rich proteins, cystatins, histatins, and mucins) preferentially adhere to the surface of the three categories of the prosthetic material investigated based on their chemical and structural characteristics of the base material to which they are adhering [16]. The specific protein make-up of the pellicle formed over the surface of each of the prosthetic materials ultimately determines how each of these materials will interact with oral microorganisms, mucosal cells and masticatory forces; consequently, influencing the clinical longevity, mucosal biocompatibility, and cariogenic/infective potential of the prosthetic restoration [17]. Pellicle development is fundamentally defined by the makeup of the proteins/mucins in the saliva, as well as by the histological characteristics of the salivary glands; therefore, allowing researchers to better understand the relationship between the different salivary gland tissues and their respective ability to produce and secrete specific types of salivary constituents [18]. A foundation in the tissue characteristics of the various types of saliva emitted from the human salivary glands will help scientists determine the appropriate material for creating prostheses through a scientifically rational and evidence-based selection process for prosthodontic materials [19].

Modern biomaterials that are used in the production of prosthetic devices such as complete dentures are comprised of heat-cured acrylic resin, cold-cured acrylic resin, soft silicone liners, yttria-stabilized tetragonal zirconia polycrystals (Y-TZP) and cobalt-chromium alloy compounds, all of which will interact in a chemically distinct family with human saliva. Acrylic resin regardless of whether it is heat or cold-cured will absorb saliva over time, which affords the acrylic resin the latent property of dimensional change along with a continuous decrease in mechanical performance [20]. Acrylic resin also would not be able to support the formation of a dental pellicle, which may expose acrylic resin to greater colonization by Candida albicans when used concurrently with patients experiencing xerostomia and thus a decreased quantity and levels of salivary antifungal proteins. Conversely, both zirconia and metal dental alloy will support the formation of dental pellicles different from those formed on those types of prosthetic dental materials with respect to their composition and the bioactivity of these pellicles; thus, these types of materials would also be less susceptible to biofilm formation under the conditions of normal salivary flow. However, the magnitude of the material-specific interactions described above will be directly related to the total amount and number of proteins in the available saliva, and the total amount and type of proteins in human saliva will be a function of the histological integrity of the glands that synthesize the saliva [21].

The minor salivary glands are those that provide the ongoing low volume of surface lubrication to the denture-bearing tissues of the upper and lower jawbones, as they are typically located in close proximity to the denture-bearing mucous membranes [22]. Histological evaluation of the minor salivary glands reveals a predominance of mucous acinar components, as relatively few serous demilunes exist, a relatively simple duct system, and a significant degree of loose connective tissue stroma, all of which imply that the primary physiologic function of the minor salivary glands is to provide ongoing topical lubrication, not to create a bolus of saliva. The histological evidence indicates that there is an ongoing decrease in the density and the basic architecture of the minor salivary glands associated with becoming older, plus the effects of mechanical irritation secondary to the prolonged use of removable prosthetics contribute to the cyclical pathophysiology of the elderly edentulous patient by way of minor salivary gland structural damage leading to reduced surface lubrication, leading to further mucosal and minor salivary gland damage secondary to reduced surface lubrication [23].

Like traditional prosthodontic rehabilitation, salivary composition plays an important role in the health of peri-implant tissue; specifically, the influence of salivary composition in relation to biofilm formation, corrosion of metallic implant components and the inflammatory mediators present in peri-implant sulcus fluid [24]. Changes in the salivary protein makeup will adversely affect the biological and mechanical life of implant-supported restorations in those patients who have exhibited hyposalivation as a result of salivary gland histological changes. In spite of the significance of the relationship between histological evaluation of the salivary glands and prosthodontic treatment, no comprehensive histomorphometric assessment has been carried out on the three major salivary glands using H&E and PAS histochemical staining and related to simultaneous measurements of salivary function and dental biomaterial criteria in one study. This study will fill the current gap in the literature and will provide a morphometric depiction of human salivary gland morphology that can be utilized by any standard histopathology laboratory and will thus represent a usable and accessible reference for the clinical histological examination of the salivary glands of the population receiving prosthodontic treatment.

MATERIALS AND METHODS

Study Design and Ethical Approval

This research was intended to be a cross-sectional study and both histomorphometric and biofunctional in nature. The study incorporated cadaveric analysis of glands, clinical analysis of live individual's saliva, and in vitro analysis of the surfaces of dental biomaterials. All study-related activities were completed in accordance with the Declaration of Helsinki as revised in 2013. Written informed consent was obtained from legal representatives of cadaveric donors before the harvesting of tissue specimens, and all living individuals who participated in the saliva collection procedures provided written informed consent. No financial benefit was provided to any individual for participating.

Collection of Cadaveric Specimens

A total of 45 specimens were collected from 15 adult human cadavers (mean age 58.3±12.7 years, 9 male and 6 female) by one trained anatomist 12 hours after the death of the individual. To be included as a donor, there must have been no reported conditions known to affect the structure and/or appearance of salivary glands as follows: (a) autoimmune conditions (e.g., Sjogrens syndrome); (b) type I or II diabetes mellitus with oral complications; (c) malignancies of the head/neck area; (d) previous radiotherapy to the face/orofacial region; (e) chronic abuse of alcohol; and

(f) advanced HIV disease. Each of the glands was dissected in its totality (with the capsule intact) utilizing established and recognized anatomical planes. Tissue blocks approximately 5×5×3 mm in size were obtained from established and recognized parenchymal areas: the central lobule of the parotid gland, the body of the submandibular gland at the midpoint of the hilum and peripheral zones of the gland, and the anterior third of the sublingual gland. Only parenchymatous tissue was obtained as samples; any examples of capsular fibrosis, intralobular deposits of adipose tissue, and hilares connective tissue were avoided in all areas.

Preparation and Sectioning of Tissue Samples

Excised tissue samples were immediately preserved using 10% neutral buffered formalin (pH 7.4) after being fixed for 48 hours at room temperature while gently stirring under continuous horizontal motion. Once completed, specimens were processed through ascending alcoholic solutions (70%, 80%, 95% and two changes of anhydrous), cleared with xylene (two changes for a 30-minute interval per change), soaked into paraffin wax through a series of steps that involved first warming the paraffin wax to 60°C inside a vacuum chamber for two hours; finally embedding into only new paraffin blocks and properly orienting the tissues in those blocks. Serial sectioning occurred from each paraffin block was performed using a rotary microtome (Leica RM2255; Leica Biosystems, Wetzlar, Germany) that had been calibrated prior to use, thus ensuring that 4 µm sections were uniformly cut. All sections were subsequently floated in a 42°C water bath before being mounted to positively charged glass (with sufficient time allotted for tissue to adhere) then placed in an incubator at 60°C for one hour before being stored at room temperature to await staining.

Haematoxylin and Eosin Stain Procedure

To perform the above staining process, sections were routinely de-paraffinized through two (5-minute) changes of xylene, followed by rehydration through descending alcohols (two-minute intervals in 100%, 95%, 80%, and 70%). Afterwards, sections were rinsed in running tap water. Sections were stained in Gill's No. 2 Heamatoxylin for eight minutes and then differentiated in 1% acid-alcohol through two dips, followed by being blued (two-minute rinse) in Scott's Tap Water Substitute, rinsed in running water, counterstained with Eosin Y at a 1% concentration (three minutes), dehydrated through ascending alcohols, cleared in xylene, and mounted under glass coverslips using DPX Mountant (Sigma-Aldrich, St. Louis, MO, USA). Consistency of staining between batches was confirmed through concurrent processing of control sections from a single reference block.H&E stained sections were used for all primary morphometrics and for the characterisation of acinar cell type, duct architecture, myoepithelial cell morphology, connective tissue composition, and adipocytic infiltration.

Periodic Acid-Schiff (PAS) Staining

Periodic acid-Schiff staining was conducted on an additional set of sections from each specimen block. Deparaffinised and rehydrated sections were treated with 1% aqueous periodic acid for 10 minutes to oxidise vicinal hydroxyl groups on polysaccharides and glycoproteins, rinsed in distilled water, immersed in Schiff reagent for 20 minutes, rinsed for 5 minutes with running tap water to develop the magenta colour, lightly counterstained with Mayer's haematoxylin, dehydrated, and finally cleared and coverslipped with DPX mountant. The PAS sections were specifically used to delineate and measure mucin-containing secretory granules in mucous acinar cells and serous demilune cells, outline the basement membrane integrity around acini and ducts, and to quantify the PAS-positive granule area per unit of acinar cell area as an index of secretory granule loading.

Histomorphometric Quantification

Morphometric analysis of the H&E and PAS-stained images was performed utilising calibrated image analysis software (ImageJ version 1.53c; National Institutes of Health, Bethesda, MD, USA) interfaced with a digital microscopy system (Olympus BX53; Olympus, Tokyo, Japan) controlled with a calibrated stage micrometer. For each specimen, 10 randomly-spaced non-overlapping high power (400×) fields of microscopic view of the parenchymal tissue were obtained from systematically randomised locations regardless of the presence of vascular or ductal tissue in the field of view.The following measurements were taken: (i) using a 100-point Merz grid and point-counting planimetry to measure the cross-sectional area at right angles across the acinar cell population (µm²); (ii) using parenchymal analysis to calculate the volume fraction of acinar cells (Vv, %) determined as% acinar cell cytoplasm compared to total area of all parenchyma excluding stroma and duct compartments; (iii) counting and identifying the serous acinar cells (% of total acinar cells); (iv) counting and identifying the mucous acinar cells (%); (v) calculating the nuclear/cytoplasmic ratio for each acinar cell; (vi) measuring the mean intercalated duct luminal diameter (µm); (vii) measuring mean striated duct luminal diameters (µm); (viii) counting and identifying the density of identifiable myoepithelial cells found when counting peripheral to the acinar basement membrane using histology (H&E) for the acinar perimeter (cells/mm²); (ix) measuring the cross-sectional area of PAS-stained secretory granule found in each acinar cell (PAS-positive) (µm²); (x) calculating total tissue volume for the connective tissue stroma as determined by the total tissue area occupied by fibrous connective tissue plus adipose connective tissue.

Measurements were repeated by the same observer on 15 random fields, 2 weeks apart, for both the primary observer and a secondary observer who was unaware of gland identity, to assess intraobserver and interobserver repeatability.

Salivary Flow Rate and Biochemical Evaluation of Saliva

Assessment of salivary function and performance was performed on a total of 60 otherwise healthy human adult subjects (mean age 34.6 ± 9.8 yrs) [32 male (53%), 28 female (47%)] from Orange County, California.

Exclusion criteria for the study were:

- Current use of medications that had previously been established to affect salivary flow,
- Diagnosed and/or treated salivary gland disease and/or surgery,
- Autoimmune disease,
- Previous radiation therapy,
- Active smoking,
- Active periodontal disease.

Unstimulated whole salivary flow rate (UWSFR) was measured using the timed spitting method over a 15-minute period into pre-weighed, sterile, graduated tubes in the morning, following a 2-hour fast, while subjects were seated and asked not to swallow, speak, or move their heads throughout the collection process. Stimulated salivary flow rate (SSFR) was measured over five minutes by chewing a piece of paraffin wax weighing 1.0 g at a rate of 60 chews per minute. Each flow rate measurement was reported as mL/min. Salivary pH was measured immediately following collection using a calibrated microelectrode pH meter (SevenGo Duo Pro; Mettler-Toledo, Columbus, OH, USA). Total protein was determined using the Bradford method. Alpha-amylase activity was quantitated by spectrophotometer using the CNPG3 substrate method. Mucin concentrations were determined using a biotinylated enzyme-linked lectin assay based on Ulex europaeus agglutinin I.

Preparation of Dental Materials and Surface Characterization

Disc specimens (10 mm diameter x 2 mm thickness; n = 5 for each test material) were manufactured from five types of dental materials:

- Heat-polymerized acrylic resin (ProBase Hot; Ivoclar Vivadent);
- Autopolymerized acrylic resin (ProBase Cold; Ivoclar Vivadent);
- Room temperature vulcanizing silicone soft liner (Molloplast-B; DETAX GmbH);
- Full contour monolithic zirconium (Katana UTML; Kuraray Noritake Dental) that were sintered in accordance with the manufacturer's instructions at 1500°C;
- Cobalt/chromium alloy (Wironit Extra-Hard; BEGO) manufactured using lost wax technique.

All specimens were polished to a standardized surface roughness arithmetic average (Ra) of 0.20 ± 0.05 µm as verified using contact profilometry (Surftest SJ-210; Mitutoyo) and were cleaned in an ultrasonic bath filled with 70% ethanol for 10 minutes, rinsed with distilled water prior to taking a baseline measurement of the contact angle. Specimens were pre-conditioned by immersion in pooled whole stimulated saliva (37 °C for 60 minutes) from five volunteers. The contact angle was measured using 2 µL of ultrapure H2O and diiodomethane droplets before and after conditioning using the sessile drop technique (DSA25E; KRÜSS GmbH, Hamburg, Germany). The Owens-Wendt-Rabel-Kaelble method was used to calculate total surface free energy and its dispersion and polar components.

Statistical Analysis

All statistical analyses were performed using IBM Statistical Package for the Social Sciences, version 26.0 (IBM Corp., Armonk, NY, USA). The Shapiro-Wilk test was performed for all continuous variables to confirm the normality of the data. One-way Analysis of Variance (ANOVA) with Tukey's HSD post-hoc test was used to assess the differences between all three types of glands for each of the histomorphometric parameters measured. Pearson correlation coefficients were used to evaluate the correlations between histomorphometric variables and salivary functional variables. Differences in the contact angle and total surface free energy measurements within each test material group were evaluated using paired t-tests; differences between materials were evaluated using one-way ANOVA with a Tukey post hoc correction. Intraobserver and interobserver reliability were evaluated using intraclass correlation coefficients (ICC; two-way random effects model). The level of statistical significance was established at 0.05 (two-tailed). All continuous data are presented as mean ± SD.

RESULTS

Intraobserver and interobserver intraclass correlation coefficients ranged from 0.87 to 0.94 for all histomorphometric measurements, demonstrating that the H&E and PAS-based quantitative methodologies used in this study were reproducible. Complete histomorphometric, salivary functional, and material surface data are presented in Tables 1–4. An illustrative photomicrograph of the parotid gland histology stained with H&E at ×40 magnification is shown in Figure 1, the submandibular gland histology stained with H&E at ×40 magnification is shown in Figure 2, the submandibular gland stained with PAS at ×40 magnification is shown in Figure 3, the sublingual gland histology stained with H&E at ×40 magnification is shown in Figure 4, and the sublingual gland stained with PAS at ×40 magnification is shown in Figure 5.

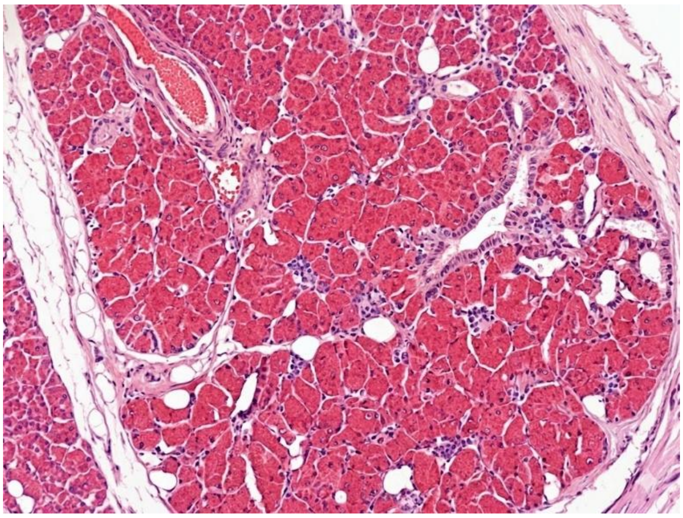

Figure 1. Histological section of parotid gland, X40, H&E

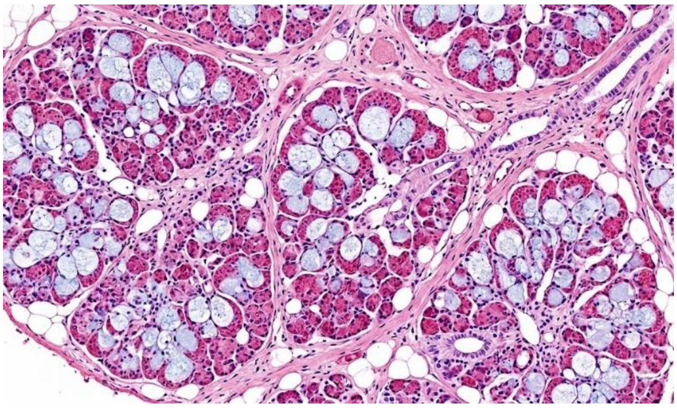

Figure 2. Histological section of submandibular gland, X 40 and H&E

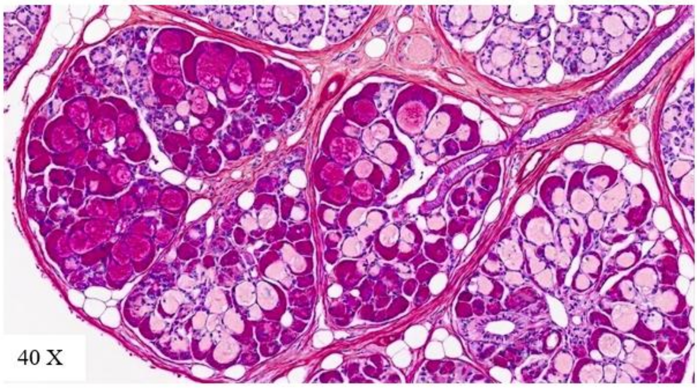

Figure 3. Histological section of submandibular gland, X 40 PAS stain

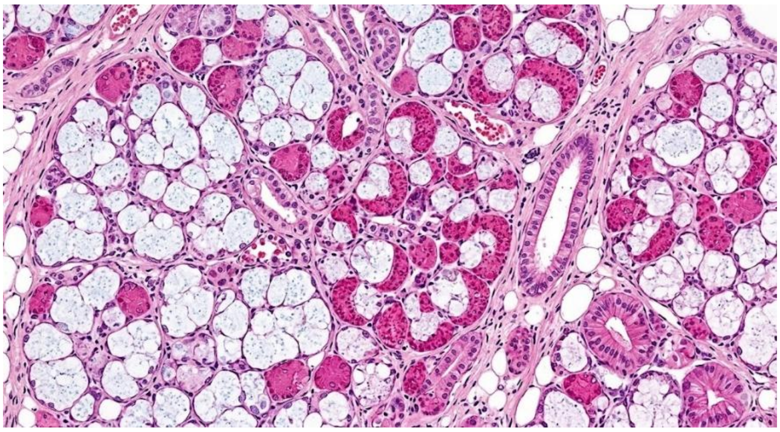

Figure 4. Histological section of sublingual gland, X 40 and H&E

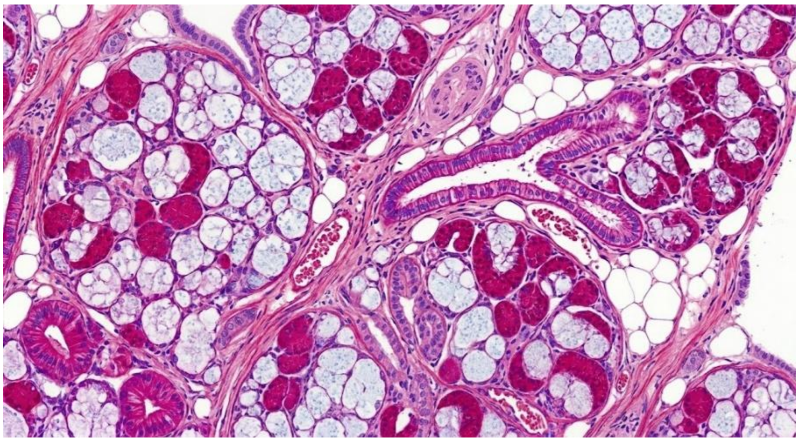

Figure 5. Histological section of sublingual gland, X 40, PAS stain

H&E- and PAS-based histomorphometric analyses showed statistically significant differences among the three major salivary glands across all 10 parameters of measurement (Table 1). The parotid gland had the largest mean cross-sectional area of acinar cells (248.3±31.4 µm²), significantly different from the submandibular (192.7±28.6 µm²) and sublingual glands (177.4±24.1 µm²; $p<0.001$ for both comparisons). The parotid gland also had the highest acinar cell volume fraction (68.4±7.2%), followed by the submandibular (61.3±6.8%) and sublingual (54.7±8.3%) glands, with each comparison yielding $p<0.001$. The serous/mucous acinar cell ratio, based on the H&E histological morphology used in this study, demonstrated the expected serous/mucous acinar cells' serous/mucous proportions between the three glands: parotid glands were 98.2±1.4% serous, submandibular glands were 62.8±8.6% serous, and sublingual glands were only 14.3±5.7% serous. The area of PAS-positive secretory granules per acinar cell progressively increased, indicating the increased density of PAS-positive mucous granules in relation to mucous specialization, from parotid (38.4±7.6 µm²), to submandibular (74.2±9.4 µm²), to sublingual (112.8±14.3 µm²). The mean width of striated ducts in the parotid and submandibular glands were significantly wider than those in the sublingual glands (the means in the parotid and submandibular were 42.7±6.3 and 38.4±5.8, respectively, versus 22.3±4.1 in sublingual glands; $p<0.001$). The greatest connective tissue stroma fraction was in the sublingual glands (29.7±6.2%), while the least was in the parotid glands (22.1±4.8%; $p=0.018$).

Table 1. Histomorphometric Parameters of Major Human Salivary Glands by H&E and PAS Staining (n=15 specimens per gland type)

Parameter	Parotid Mean±SD	Submandibular Mean±SD	Sublingual Mean±SD	p-value
Acinar cell cross-sectional area (µm²)	248.3±31.4	192.7±28.6[a]	177.4±24.1[ab]	<0.001
Acinar cell volume fraction (Vv, %)	68.4±7.2	61.3±6.8[a]	54.7±8.3[ab]	<0.001
Serous acinar cell proportion (%)	98.2±1.4	62.8±8.6[a]	14.3±5.7[ab]	<0.001
Mucous acinar cell proportion (%)	1.8±1.4	37.2±8.6[a]	85.7±5.7[ab]	<0.001
Nuclear-to-cytoplasmic ratio	0.18±0.03	0.22±0.04[a]	0.26±0.05[ab]	0.003
Intercalated duct lumen diameter (µm)	12.4±2.1	10.8±1.9	8.6±1.7[ab]	0.001
Striated duct lumen diameter (µm)	42.7±6.3	38.4±5.8	22.3±4.1[ab]	<0.001
Myoepithelial cell density (cells/mm²)	184.6±22.3	176.8±19.7	148.3±17.6[ab]	0.012
PAS-positive granule area per acinar cell (µm²)	38.4±7.6	74.2±9.4[a]	112.8±14.3[ab]	<0.001
Connective tissue stroma fraction (%)	22.1±4.8	25.4±5.3	29.7±6.2[a]	0.018

Values are Mean±SD. [a]Significantly different from parotid (p<0.05, Tukey post-hoc). [b]Significantly different from submandibular (p<0.05, Tukey post-hoc). PAS: periodic acid-Schiff; Vv: volume fraction.

The summary of salivary flow rate and biochemical parameters is presented in Table 2. The average Unstimulated Whole Saliva Flow Rate (UWSFR) was 0.38±0.14mL/min, and the average Stimulated Saliva Flow Rate (SSFR) was 1.72±0.47mL/min, which showed a large range of variability from one subject to the next. Of the 60 subjects, 14 (23.3%) had UWSFRs less than 0.25mL/min, therefore fitting the criteria for hyposalivation. Total protein concentration was 2.84±0.63mg/mL, alpha amylase activity was 142.7±38.4U/mL, and mucin concentration was 0.87±0.22mg/mL.

Table 2. Salivary Flow Rates and Biochemical Composition in Healthy Adult Volunteers (n=60)

Parameter	Mean±SD	Published Reference Range
Unstimulated whole salivary flow rate (mL/min)	0.38±0.14	0.25–0.35[a]
Stimulated whole salivary flow rate (mL/min)	1.72±0.47	1.00–2.00[a]
Salivary pH	7.12±0.38	6.75–7.25[a]
Total protein concentration (mg/mL)	2.84±0.63	1.80–3.60[a]
Alpha-amylase activity (U/mL)	142.7±38.4	80.0–200.0[a]
Mucin concentration (mg/mL)	0.87±0.22	0.50–1.20[a]

[a]*Reference ranges from* [25]. *UWSFR: unstimulated whole salivary flow rate; SSFR: stimulated whole salivary flow rate.*

The five types of dental materials showed significant decreases in water contact angles and corresponding increases in surface energy after being conditioned with saliva. This indicates that pellicles formed on all five materials. Postconditioning, zirconia had the most hydrophilic surface, with a contact angle of 28.4±3.2° and a surface energy of 58.4±4.2 mJ/m², while the silicone soft liner had the most hydrophobic surface, with a contact angle of 73.2±8.4° and a surface energy of 29.7±3.3 mJ/m². The alloy (AA) produced the largest decrease in contact angle (ΔCA = -18.1°), and all intermaterial differences in postconditioning contact angles and surface energies were statistically significant ($p<0.001$, one-way ANOVA).

Table 3. Contact Angle (CA) and Surface Free Energy (SFE) of Dental Materials Before and After 60-Minute Salivary Conditioning

Material	CA Pre (°)	CA Post (°)	ΔCA (°)	SFE Pre (mJ/m²)	SFE Post (mJ/m²)	p
Heat-polymerized acrylic resin	72.4±5.8	54.7±6.1	-17.7	34.2±3.8	42.8±4.1	<.001
Autopolymerized acrylic resin	76.8±6.3	61.3±5.8	-15.5	31.7±3.4	39.4±3.9	<.001
Silicone soft liner (RTV)	89.4±7.2	73.2±8.4	-16.2	22.1±2.9	29.7±3.3	<.001
Monolithic zirconia	44.3±4.6	28.4±3.2	-15.9	48.6±4.8	58.4±4.2	<.001
Cobalt-chromium alloy	52.7±5.1	34.6±4.1	-18.1	43.8±4.3	54.1±4.7	<.001

RTV: room-temperature-vulcanized silicone. p: paired t-test (pre vs. post within material). Inter-material post-conditioning differences all $p<0.001$ (one-way ANOVA, Tukey post-hoc).

The Pearson correlation analyses between the histomorphometric parameters derived from H&E and PAS staining and functional outcomes of salivary function are summarized in table 4. The strongest correlation of the various histomorphometric variables was the proportion of serous acini cells to amylase activity ($r=0.73$, $p<0.001$), while the proportion of mucous acini cells was the highest correlation with mucin concentration ($r=0.79$, $p<0.001$). The acinar cell volume fraction also had a statistically significant correlation with both SSFR ($r=0.72$, $p<0.001$) and total protein ($r=0.64$, $p<0.001$). The area of PAS-positive granules per acinus also showed the strongest correlation with mucin concentration ($r=0.71$, $p<0.001$). The connective tissue to stroma fraction had significant although inverse correlations with SSFR ($r=-0.48$, $p<0.05$) and total protein ($r=-0.39$, $p<0.05$), suggesting that more replacement of stroma within glands resulted in a decrease of secretory output from the glands.

Table 4. Pearson Correlation Coefficients Between H&E/PAS Histomorphometric Parameters and Salivary Functional Outcomes

H&E/PAS Histomorphometric Parameter	SSFR (r)	Total Protein (r)	Amylase (r)	Mucin Conc. (r)
Acinar cell volume fraction (Vv)	0.72**	0.64**	0.69**	0.46*

H&E/PAS Histomorphometric Parameter	SSFR (r)	Total Protein (r)	Amylase (r)	Mucin Conc. (r)
Acinar cell cross-sectional area	0.65**	0.58**	0.62**	0.39*
Serous acinar cell proportion	0.68**	0.61**	0.73**	0.17
Mucous acinar cell proportion	0.21	0.46*	0.14	0.79**
PAS-positive granule area per acinar cell	0.43*	0.52**	0.31	0.71**
Myoepithelial cell density	0.57**	0.42*	0.51**	0.46*
Striated duct lumen diameter	0.51**	0.44*	0.48*	0.30
Connective tissue stroma fraction	-0.48*	-0.39*	-0.44*	-0.27

***p<0.01; *p<0.05. SSFR: stimulated whole salivary flow rate. Mucin Conc.: mucin concentration determined by lectin assay.*

DISCUSSION

The results of this investigation establish that quantitative H&E and PAS histomorphometric analysis of human salivary glands yields clinically meaningful indices of secretory function that correlate significantly with paired salivary flow rates and biochemical parameters. This validation of routine histological staining as a functional proxy carries direct practical implications, since H&E and PAS-based assessment is universally available in clinical histopathology laboratories and does not require specialised reagents or molecular techniques. The ability to predict functional salivary output from tissue morphometry strengthens the rationale for incorporating salivary gland biopsy-particularly of the readily accessible minor labial glands, which share the histological organisation principles of the major glands into the diagnostic workup of prosthodontic patients presenting with xerostomia or unexplained prosthetic instability [26,27].

The inter-glandular morphometric differences in acinar cell cross-sectional area, with the parotid gland exhibiting cells nearly 40% larger in cross-section than sublingual acinar cells, reflect fundamental differences in the secretory machinery rather than simply gland size [28]. Parotid serous acinar cells require extensive rough endoplasmic reticulum and Golgi apparatus for the synthesis, packaging, and transport of alpha-amylase and other serous proteins, and this biosynthetic infrastructure contributes substantially to their larger cytoplasmic volume as seen on H&E [29]. The strong positive correlation between serous acinar cell proportion and amylase activity (r=0.73) confirms that this morphological parameter faithfully tracks the enzyme-secreting capacity of the gland at the individual subject level. In conditions characterised by progressive serous acinar atrophy-most notably Sjogren's syndrome type A and parotid irradiation injury the H&E observation of reduced serous acini would therefore directly predict the reduction in stimulated salivary amylase output that impairs dietary carbohydrate digestion and alters the biochemical environment at the interface between saliva and prosthetic materials [30,31].

The inverse relationship between mucous acinar cell proportion and serous cell proportion across the three glands, combined with the strong correlation between mucous acinar proportion and mucin concentration (r=0.79), provides morphometric confirmation of the established histological basis for the differential viscosity of glandular secretions. The sublingual gland, with 85.7% mucous acini on H&E assessment, produces the most viscous and adhesive salivary fraction, and the high PAS-positive granule area per acinar cell (112.8±14.3 µm²) in this gland reflects the abundant neutral glycoprotein content of mucous secretory granules that stain intensely magenta with the PAS reaction [10]. This histological correlate of mucin-rich secretion is directly relevant to denture retention mechanics, as the mucin-mediated viscoelastic film generated by submandibular and sublingual contributions is the principal source of the capillary adhesive force that stabilises complete dentures against vertical displacement during function [12,13]. Clinical evidence consistently demonstrates that patients whose submandibular and sublingual glands show histological signs of mucous acinar atrophy-including reduction in volume fraction, nuclear-to-cytoplasmic ratio inversion, and diminished PAS granule loading-experience significantly greater difficulty with complete denture stability than patients with preserved glandular architecture [14,23].

The quantitative relationship between striated duct lumen diameter and salivary flow rate (r=0.51, p<0.01) identified in the present correlation analysis is a histologically novel finding that may reflect a structural-functional coupling between ductal calibre and flow capacity analogous to that described for other exocrine organs. Striated ducts, distinguishable on H&E by their tall columnar eosinophilic epithelium and basal striations, serve as the principal sites of ionic modification in the salivary duct system and their luminal calibre likely reflects the cumulative secretory output from the acinar units they drain [7]. Glands with larger acinar volume fractions and greater secretory cell mass would be expected to require larger ductal lumina to accommodate higher secretory volumes, and the present morphometric data support this structural rationale. This correlation suggests that striated duct diameter, measurable with high reproducibility on standard H&E sections, could serve as a secondary morphometric indicator of glandular secretory capacity

ejprd.org - Published by Riset Publishing Services LLC.

in circumstances where acinar identification is rendered difficult by fibrotic or atrophic changes.

The significant inverse correlation between connective tissue stroma fraction and salivary flow rate (r=-0.48) documented in the present study provides quantitative morphometric support for the clinical observation that glandular fibrosis and fatty infiltration reduce secretory output. On H&E sections, the replacement of functional acinar parenchyma by fibrous stroma or adipocytes is the most visible indicator of glandular pathology in conditions such as age-related glandular involution, post-irradiation fibrosis, and chronic sialadenitis [8]. The finding that even in the non-pathological cadaveric specimens in the present cohort-which were screened to exclude overt glandular disease connective tissue stroma fraction varied from 22.1% to 29.7% across gland types and correlated inversely with functional output, indicates that the stroma-to-parenchyma ratio on H&E is a continuously variable, functionally meaningful parameter rather than a binary normal/abnormal indicator. This has practical implications for histopathological reporting of salivary gland biopsies in prosthodontic patients: a quantified stroma fraction, rather than a qualitative descriptor, would provide more clinically actionable information about residual secretory capacity [26].

The PAS staining data merit separate discussion, as the quantification of PAS-positive granule area per acinar cell as a morphometric parameter represents a methodological contribution of the present study. The progressive increase in this parameter from parotid (38.4 μm²) to submandibular (74.2 μm²) to sublingual (112.8 μm²) glands reflects the dominant contribution of mucous glycoproteins to the PAS-reactive pool in each gland, since neutral mucins are the most intensely PAS-positive cytoplasmic constituent in salivary cells [32]. However, PAS positivity in parotid sections, while quantitatively lower, is not negligible-it reflects the glycoprotein content of serous secretory granules, basement membrane integrity around acini and ducts, and the modest glycoprotein complement of ductal cells. The correlation between PAS granule area and mucin concentration (r=0.71) validates this parameter as a morphometric surrogate for the mucin secretory load of a gland and could be employed in diagnostic biopsies to estimate the degree of mucous versus serous secretory specialisation independently of acinar cell morphological classification on H&E alone.

With regard to the dental material surface characterisation findings, the differential wettability responses to salivary conditioning across the five material categories demonstrate that material substrate chemistry fundamentally determines pellicle adsorption, irrespective of standardised surface roughness [33,34]. The superior post-conditioning hydrophilicity of zirconia, with the lowest contact angle (28.4°) and highest surface free energy (58.4 mJ/m²), has direct implications for its intraoral biological performance. High surface wettability reflects a thick, well-organised salivary pellicle whose protein constituents include antimicrobial and anti-adhesive molecules that reduce initial microbial colonisation [35]. For prosthodontic applications, this translates to a potentially lower incidence of peri-prosthetic biofilm formation and a more favourable early tissue cell response on zirconia components compared to polymer alternatives. The contrasting behaviour of silicone soft liners retaining the highest contact angle and lowest surface energy after salivary conditioning reflects the hydrophobic polydimethylsiloxane backbone of this material class, which presents minimal sites for electrostatic or hydrogen-bond interactions with salivary protein domains [19]. The clinical consequence is impaired pellicle formation, reduced incorporation of salivary antimicrobial peptides at the liner surface, and the well-documented susceptibility of silicone soft liners to Candida colonisation in patients whose salivary antifungal defences are already compromised by reduced flow [36].

The finding that 23.3% of otherwise healthy volunteers demonstrated UWSFR below the clinical hyposalivation threshold of 0.25 mL/min, without subjective awareness, reinforces the importance of objective salivary flow measurement as a routine component of prosthodontic diagnostic assessment. The histological data from the present study provide the mechanistic background for this subclinical hyposalivation: the acinar volume fraction of the submandibular and sublingual glands, which are the dominant contributors to resting salivary flow, is continuously variable among individuals, and even moderate reductions in this parameter would be predicted from the correlation data to produce measurable reductions in flow rate [37]. This suggests that routine H&E-based morphometric assessment of minor salivary gland biopsies could complement objective flow measurements in the pre-prosthetic evaluation of patients with suspected hyposalivation, providing histological insight into the structural basis of their salivary deficit that would inform both prognosis and treatment planning [26,28,35].

Several study limitations should be acknowledged. The cadaveric tissue specimens were sourced from a different cohort than the living salivary function volunteers, precluding direct within-subject histology-to-function correlation, which remains the methodological ideal for this research question. The cadaveric cohort was older (mean age 58.3 years) than the living cohort (mean age 34.6 years), introducing a potential confound given the age-related decline in acinar cell volume fraction and increase in stroma fraction documented in salivary glands [8]. The dental material pellicle formation protocol, conducted over 60 minutes in pooled stimulated saliva, represents a single time point in the dynamic pellicle maturation process and does not capture the compositional evolution of the pellicle over clinical time scales of hours to days [38,39]. Future prospective studies should address these limitations by incorporating minor salivary gland biopsy paired with salivary functional measurements within the same prosthodontic patient cohort, enabling direct validation of the histomorphometric predictors of function in the population for whom these data are clinically intended.

CONCLUSION

A quantitative histomorphometric analysis using H&E only and PAS only stained sections of the three major salivary glands provides clinically relevant indices of salivary gland secretory capacity that correlate significantly with paired measurements of salivary flow rate and biochemical composition. The acinar cell volume fraction, ratio of serous to mucous acinar cells, area of PAS-positive granules per acinar cell, striated duct lumen diameter, and fraction of connective tissue stroma provide a histological profile that predicts salivary functional output by using staining techniques routinely used in clinical histopathology. The characterisation of the dental material surface further demonstrates that the formation of the salivary pellicle significantly affects the surface energy of all types of conventional prosthodontic materials where zirconia has the highest hydrophilicity and silicone soft liners have the lowest post-conditioning. Therefore, these findings provide a basis for routine staining histology for the understanding of how abnormalities in the parenchymal architecture of the salivary gland due to aged and/or diseased or due to iatrogenic injury may cause impairment of prosthetic retention, reduced mucosal tolerance, and alteration of biomaterial surface biology. Therefore, the objective measurement of salivary flow rates and, if indicated, a minor salivary gland biopsy with H&E and PAS morphometric data, should be included in the pre-prosthetic diagnostic process for patients with known or suspected salivary hypofunction.

REFERENCES

1. Amerongen AN, Veerman E. Saliva–the defender of the oral cavity. Oral diseases. 2002;8(1):12–22.
2. Humphrey SP, Williamson RT. A review of saliva: normal composition, flow, and function. The Journal of prosthetic dentistry. 2001;85(2):162–9.
3. Tandler B. Ultrastructure of the human submaxillary gland. I. Architecture and histological relationships of the secretory cells. Am J Anat. 1962 Nov;111(3):287–307. doi:10.1002/aja.1001110304
4. Young JA, Van Lennep EW. The morphology of salivary glands. (No Title) [Internet]. 1978 [cited 2026 Apr 4]. Available from: https://cir.nii.ac.jp/crid/1970867909823857550
5. Hand AR, Pathmanathan D, Field RB. Morphological features of the minor salivary glands. Archives of oral biology. 1999;44:S3–10.
6. Chibly AM, Aure MH, Patel VN, Hoffman MP. Salivary gland function, development, and regeneration. Physiological Reviews. 2022 Jul 1;102(3):1495–552. doi:10.1152/physrev.00015.2021
7. Pedersen AML, Sørensen CE, Proctor GB, Carpenter GH, Ekström J. Salivary secretion in health and disease. J of Oral Rehabilitation. 2018 Sep;45(9):730–46. doi:10.1111/joor.12664
8. Ship JA, Pillemer SR, Baum BJ. Xerostomia and the Geriatric Patient. J American Geriatrics Society. 2002 Mar;50(3):535–43. doi:10.1046/j.1532-5415.2002.50123.x
9. Proctor GB, Carpenter GH. Regulation of salivary gland function by autonomic nerves. Autonomic Neuroscience. 2007;133(1):3–18.
10. McManus JFA. Histological and Histochemical Uses of Periodic Acid. Stain Technology. 1948 Jan;23(3):99–108. doi:10.3109/10520294809106232
11. Tabak LA. In defense of the oral cavity: structure, biosynthesis, and function of salivary mucins. Annual review of physiology. 1995;57(1):547–64.
12. Inoue H, Ono K, Masuda W, Inagaki T, Yokota M, Inenaga K. Rheological properties of human saliva and salivary mucins. Journal of Oral Biosciences. 2008;50(2):134–41.
13. Tabak LA, Levine MJ, Mandel ID, Ellison SA. Role of salivary mucins in the protection of the oral cavity. J Oral Pathology Medicine. 1982 Jan;11(1):1–17. doi:10.1111/j.1600-0714.1982.tb00138.x
14. Sreebny LM, Schwartz SS. A reference guide to drugs and dry mouth – 2nd edition. Gerodontology. 1997 Jul;14(1):33–47. doi:10.1111/j.1741-2358.1997.00033.x
15. Hannig C, Hannig M. The oral cavity—a key system to understand substratum-dependent bioadhesion on solid surfaces in man. Clin Oral Invest. 2009 Jun;13(2):123–39. doi:10.1007/s00784-008-0243-3
16. Siqueira WL, Custodio W, McDonald EE. New Insights into the Composition and Functions of the Acquired Enamel Pellicle. J Dent Res. 2012 Dec;91(12):1110–8. doi:10.1177/0022034512462578
17. Scannapieco FA. Saliva-Bacterium Interactions in Oral Microbial Ecology. Critical Reviews in Oral Biology & Medicine. 1994 Sep;5(3):203–48. doi:10.1177/10454411940050030201
18. Anusavice KJ, Shen C, Rawls HR. Phillips' science of dental materials [Internet]. Elsevier Health Sciences; 2012 [cited 2026 Apr 4]. Available from: https://books.google.com/books?hl=en&lr=&id=gzUeKDhP-KQC&oi=fnd&pg=PP1&dq=19.%09Anusavice+KJ,+Shen+C,+Rawls+HR.+Phillips%27+Science+of+Dental+Materials.+12th+ed.+St.+Louis:+Elsevier+Saunders%3B+2013.&ots=BiR_q9JKp-&sig=KQEuHX-xjrAjejUItBP7M5lEX74
19. Nikawa H, Hamada T, Yamamoto T. Denture plaque—past and recent concerns. Journal of dentistry. 1998;26(4):299–304.
20. Al-Radha ASD, Dymock D, Younes C, O'Sullivan D. Surface properties of titanium and zirconia dental implant materials and their effect on bacterial adhesion. Journal of dentistry. 2012;40(2):146–53.
21. Fox RI. Sjögren's syndrome. The Lancet. 2005;366(9482):321–31.
22. Müller F, Naharro M, Carlsson GE. What are the prevalence and incidence of tooth loss in the adult and elderly population in Europe? Clinical Oral Implants Res. 2007 Jun;18(s3):2–14. doi:10.1111/j.1600-0501.2007.01459.x
23. Salvi GE, Lawrence HP, Offenbacher S, Beck JD. Influence of risk factors on the pathogenesis of

periodontitis. Periodontology 2000. 1997 Jun;14(1):173–201. doi:10.1111/j.1600-0757.1997.tb00197.x
24. Gittens RA, Olivares-Navarrete R, Schwartz Z, Boyan BD. Implant osseointegration and the role of microroughness and nanostructures: lessons for spine implants. Acta biomaterialia. 2014;10(8):3363–71.
25. Pedersen AML, Sørensen CE, Proctor GB, Carpenter GH, Ekström J. Salivary secretion in health and disease. J of Oral Rehabilitation. 2018 Sep;45(9):730–46. doi:10.1111/joor.12664
26. Baum BJ. Principles of Saliva Secretion. Annals of the New York Academy of Sciences. 1993 Sep;694(1):17–23. doi:10.1111/j.1749-6632.1993.tb18338.x
27. Thomson WM. Issues in the epidemiological investigation of dry mouth. Gerodontology. 2005 Jun;22(2):65–76. doi:10.1111/j.1741-2358.2005.00058.x
28. Vissink A, Jansma J, Spijkervet FKL, Burlage FR, Coppes RP. Oral sequelae of head and neck radiotherapy. Critical Reviews in Oral Biology & Medicine. 2003;14(3):199–212.
29. Aps JK, Martens LC. The physiology of saliva and transfer of drugs into saliva. Forensic science international. 2005;150(2–3):119–31.
30. Guggenheimer J, Moore PA. Xerostomia: etiology, recognition and treatment. The journal of the american dental association. 2003;134(1):61–9.
31. Hannig M, Hannig C. Nanomaterials in preventive dentistry. Nature nanotechnology. 2010;5(8):565–9.
32. Sadamori S, Ishii T, Hamada T. Influence of thickness on the linear dimensional change, warpage, and water uptake of a denture base resin. The International Journal of Prosthodontics. 1997;10(1):35–43.
33. Pröbster L, Geis-Gerstorfer J, Kirchner E, Kanjantra P. *In vitro* evaluation of a glass–ceramic restorative material. J of Oral Rehabilitation. 1997 Sep;24(9):636–45. doi:10.1111/j.1365-2842.1997.tb01075.x
34. Rykke M, Young A, Smistad G, Rölla G, Karlsen J. Zeta potentials of human salivary micelle-like particles. Colloids and Surfaces B: Biointerfaces. 1996;6(1):51–6.
35. Fox PC, Bowman SJ, Segal B, Vivino FB, Murukutla N, Choueiri K, et al. Oral involvement in primary Sjögren syndrome. The Journal of the American Dental Association. 2008;139(12):1592–601.
36. Dodds MW, Johnson DA, Yeh CK. Health benefits of saliva: a review. Journal of dentistry. 2005;33(3):223–33.
37. Ozkan Y, Özcan M, Kulak Y, Kazazoglu E, Arikan A. General health, dental status and perceived dental treatment needs of an elderly population in Istanbul: General health, dental status and dental treatment needs of elderly. Gerodontology. 2011 Mar;28(1):28–36. doi:10.1111/j.1741-2358.2010.00363.x
38. Delporte C, Bryla A, Perret J. Aquaporins in salivary glands: from basic research to clinical applications. International journal of molecular sciences. 2016;17(2):166.
39. Löe H. Oral hygiene in the prevention of caries and periodontal disease. International Dental Journal. 2000 Jun;50(3):129–39. doi:10.1111/j.1875-595X.2000.tb00553.x